PHYSICAL REVIEW A VOLUME 25, NUMBER 2 FEBRUARY 1982

Ionization, excitation, and charge transfer for impacts of H^+, Li^{3+}, B^{5+}, C^{6+}, and Si^{14+} ions on atomic hydrogen

Hiroshi Ryufuku
Tokai Research Establishment, Japan Atomic Energy Research Institute, Tokai-mura, Naka-gun, Ibaraki 319-11, Japan
(Received 10 March 1981)

Unitarized-distorted-wave-approximation calculations based on a complete set of channels are performed to obtain ionization, excitation, and charge-transfer cross sections for impacts of H^+, Li^{3+}, B^{5+}, C^{6+}, and Si^{14+} ions on atomic hydrogen. The ionization channels are represented by Coulomb wave functions centered on the projectiles to account for "charge transfer to the continuum". The ionization cross sections depend less than in a quadratic relationship on projectile charge. The inclusion of ionization and excitation channels makes charge-transfer cross sections considerably smaller for higher values of the projectile charge at impact energies above 10 keV/amu. A new scaling rule to charge-transfer cross sections is discussed in comparison with experiments and other theories for the energy range 0.01 – 5000 keV/amu.

I. INTRODUCTION

Investigations on charge-transfer and ionization processes involving heavy multicharged ions and atomic hydrogen have recently received appreciable attention in connection with the practical applications to fusion research. Much work on the charge-transfer processes of this type has been reported by many theoretical and experimental investigators as summarized in Refs. 1 and 2. However, little work has been reported on the ionization and excitation processes as described in Ref. 2.

Theoretical approaches which give the charge-transfer cross sections comparatively close to experimental values are the method of coupled molecular orbitals[3–6] for the low-energy region, a classical-trajectory Monte Carlo method[7] for the intermediate-energy region, and a unitarized-distorted-wave approximation (UDWA)[8–11] for the low-, intermediate-, and high-energy regions, where low energy denotes ion-impact energy below 10 keV/amu, intermediate energy that of 10 – 100 keV/amu, and high energy that above 100 keV/amu. The recent remarkable studies are as follows.

Goffe *et al.*[12] have measured charge-transfer cross sections for collisions of fully stripped B, C, and N ions with atomic hydrogen. The ion energies are 750 – 2500 keV for the B^{5+} impact, 1380 – 2500 keV for the C^{6+} impact, and 170 keV/amu for the N^{7+} impact. They have shown that the cross sections predicted with the classical-trajectory Monte Carlo method[7] agree roughly with the measured value but exhibit a somewhat different energy dependence and that while the UDWA theory[9] leads to cross sections which are too large, the predicted energy dependence is in good agreement with the experiment.

Seim *et al.*[13] have measured cross sections for charge transfer in collisions of Li^{3+} ions with atomic hydrogen in the energy range 1.3 – 6 keV/amu. Above 2.3 keV/amu their data are in good agreement with the UDWA theory while there is a discrepancy at the lower energies.

Crandall *et al.*[14] have obtained charge-transfer cross sections for collisions of $Xe^{q+}(2 \leq q \leq 12)$, $Ar^{q+}(2 \leq q \leq 9)$, and $Fe^{q+}(q = 5,6)$ with atomic hydrogen, at low energies between 0.05 and 5 keV/amu. Their data show that the cross sections increase less than linearly with q for higher q.

Salop and Olson[15] have calculated charge-transfer cross sections for $Fe^{26+} + H$ collisions at Fe^{26+} energies of 0.2, 1.3, and 5.2 keV/amu with the method of coupled molecular states. These results, in combination with their cross sections[3,4] for impacts of C^{6+} and O^{8+}, show that the cross

sections increase more than linearly with the charge of ions at the ion-impact energy of 2.5 keV/amu.

Total ionization cross sections calculated using the Born approximation[16] show an excellent agreement with experimental values[17–19] for $H^+ + H$ collisions. However, energy and angular distributions of electrons ejected from molecular hydrogen measured by Rudd *et al.*[20] are different from the results of the Born approximation scaled to molecular hydrogen. Forward ejections are most pronounced when the velocity of the ejected electron is close to that of the projectile and show a "cusp-shaped peak" in energy distributions. Macek[21] termed the mechanism proposed in this connection "charge exchange to a continuum state."

Systematic theoretical investigations for ionization of atomic hydrogen by impact of multicharged ions have been performed by Olson and Salop[7] and by Janev and Presnyakov.[22] Olson and Salop have calculated cross sections for impacts of ions having the charge $Z=1-40$ on atomic hydrogen using the classical-trajectory Monte Carlo method. Janev and Presnyakov have considered ionization for impacts of ions of $Z=1-32$ with a dipole-approximation close-coupling calculation based on atomic orbitals.

Excitations of atomic hydrogen by impact of multicharged ions have been treated by Janev and Presnyakov[22] for the charges of ions being $Z=1-10$ and the principal quantum numbers of excited levels being $n=2-5$ with the above-stated method.

In the present work, UDWA calculations are performed using a complete set of channels including ionization, excitation, and charge-transfer channels. Ionization states are represented by Coulomb wave functions centered on the projectile as in charge-transfer calculations. Therefore, this treatment completely accounts for "charge transfer to the continuum."

Numerical calculations are carried out for impacts of H^+, Li^{3+}, B^{5+}, C^{6+}, and Si^{14+} on atomic hydrogen at impact energies $E \geq 10$ keV/amu, since charge transfer is a dominant process for impact energies $E < 10$ keV/amu and the cross sections obtained in the previous work[8–11] receive little change with the inclusion of ionization and excitation channels.

A scaling procedure for charge-transfer cross sections with respect to the energy and charge of projectiles has been obtained in the previous work[10] with neglect of ionization and excitation channels. This is improved based on the new UDWA cross sections. The new scaling rule for energy range 0.01–5000 keV/amu is discussed in comparison with experiments and other theories including the recent studies described above. Atomic units are used throughout the present paper unless otherwise stated.

II. UDWA FORMULA

The details of the derivation of the UDWA formula have been described previously[9] and only the summary will be presented here. We use the straightline trajectory impact-parameter approximation. The cross section for the transition from the initial state $|0\rangle$ to the final state $|n\rangle$ is given by

$$\sigma_n = 2\pi \int_0^\infty P_n(\rho)\rho\, d\rho \,, \tag{2.1}$$

with

$$P_n(\rho) = |\langle n | S^{\rm int} | 0 \rangle|^2 \tag{2.2}$$

and

$$S^{\rm int} = T \exp\left[-i \int_{-\infty}^{\infty} \hat{H}^{\rm int}(t) dt\right] , \tag{2.3}$$

where $P_n(\rho)$ is the transition probability for a given impact parameter ρ, $S^{\rm int}$ the S matrix in the interaction representation and $\hat{H}^{\rm int}(t)$ the interaction matrix for a given time t:

$$\hat{H}^{\rm int}(t) = \exp\left[i \int_{-\infty}^{t} H^0 dt\right] H^{\rm int} \times \exp\left[-i \int_{-\infty}^{t} H^0 dt\right] , \tag{2.4}$$

with

$$H^{\rm int} = H - H^0 \,. \tag{2.5}$$

The matrix element of H is given by

$$h_{nm} = \left[\xi_{n'} \left[\mathscr{H} - i\frac{\partial}{\partial t}\right] \xi_m\right] , \tag{2.6}$$

where $\{\xi_n\}$ is the basis set and $\mathscr{H}$ the total Hamiltonian of the collision system, and H^0 is the diagonal part of H.

The first term in expansion series of the exponential function of Eq. (2.3) is expressed as

$$t_{n0} = \int_{-\infty}^{\infty} \langle n | \hat{H}^{\rm int}(t) | 0 \rangle dt \,, \tag{2.7}$$

which can be approximated by

$$t_{n0}=\int_{-\infty}^{\infty} dt(h_{n0}-s_{n0}h_{00}) \times \exp\left[i\int_{-\infty}^{t}(h_{nn}-h_{00})dt\right], \quad (2.8)$$

with

$$s_{nm}=[\xi_{n'}\xi_m]\,. \quad (2.9)$$

Equation (2.8) is equivalent to the semiclassical distorted-wave Born-approximation (DWBA) formula[23] of the transition matrix elements.

The DWBA transition probability given by

$$p=\sum_{n=1}^{N}|t_{n0}|^2\,, \quad (2.10)$$

where $\{|n\rangle;n=0,1,2,\ldots,N\}$ denotes all channels involved in the reaction, exceeds unity not only at low-collision energies, but also even at high energies for high values of the projectile charge; that is, $S^{\rm int}$ is not unitary in the DWBA. Unitary approximation to $S^{\rm int}$ matrix may not be unique. The unitarized-distorted-wave approximation (UDWA) is a unitarization of the DWBA.

The UDWA formula is obtained by the approximation in which the chronological-ordering operator T and all matrix elements, except those involving the initial state $|0\rangle$ in the expansion series of Eq. (2.3), are ignored. Thus, in the UDWA the matrix $S^{\rm int}$ is expressed as

$$\langle 0|S^{\rm int}|0\rangle=\cos p^{1/2}\,, \quad (2.11)$$

and

$$\langle n|S^{\rm int}|0\rangle=-it_{n0}p^{-1/2}\sin p^{1/2}\quad (n\neq 0)\,. \quad (2.12)$$

It is clear from Eqs. (2.10)–(2.12) that

$$\sum_{n=0}^{N}|\langle n|S^{\rm int}|0\rangle|^2=1\,, \quad (2.13)$$

that is, the unitarity of $S^{\rm int}$ is maintained.

As described above, in the UDWA all off-diagonal matrix elements $\{t_{nn'}\}$ except those including the initial state, are ignored. Therefore, the UDWA formula cannot be applied to the processes in which transitions via some other intermediate states are dominant as in the cases of excitation and ionization at low energies. The neglect of $\{t_{nn'}\}$ implies the omission of all even order terms in $H^{\rm int}$ from the expansion of the S matrix. In the case of charge transfer, the importance of the second-order Born term has been discussed recently.[24] Although our expansion is not the plane-wave Born series, the effect of even-order terms which necessarily contain $t_{nn'}$, is left to be examined. The error introduced by the omission of the T operator has been estimated to be less than 30% in the case of the two-state problem.[8] However, this effect when $t_{nn'}$ is included is not lucite at the present time, especially at low energies. Further discussion on this approximation method will appear near future.

III. COMPUTATIONAL METHODS

Methods to calculate DWBA matrices t_{n0}, given by Eq. (2.8), are described here. For the excitation, charge-transfer, and ionization channel wave functions we use the moving atomic orbitals given by

$$\xi_n^A(\vec{r},t)=\phi_n^A(\vec{r}_A)e^{-i\vec{v}\cdot\vec{r}/2}\,, \quad (3.1a)$$

$$\xi_n^B(\vec{r},t)=\phi_n^B(\vec{r}_B)e^{i\vec{v}\cdot\vec{r}/2}\,, \quad (3.1b)$$

and

$$\xi_\nu^B(\vec{r},t)=\psi_\nu^B(\vec{r}_B)e^{i\vec{v}\cdot\vec{r}/2}\,, \quad (3.1c)$$

respectively, where A and B stand for the target nucleus (charge Z_A) and the projectile (charge Z_B), respectively, $\vec{r}_A$, $\vec{r}_B$ and $\vec{r}$ are the position vectors of the electron relative to A, B, and the midpoint of A and B, respectively, and $\phi_n^A(\vec{r}_A)$ and $\phi_n^B(\vec{r}_B)$ are hydrogenlike wave functions of the system A + electron and B + electron having negative eigenenergies ω_n^A and ω_n^B, respectively. $\psi_\nu^B(\vec{r}_B)$ is a Coulomb wave function of the system B + electron having a positive eigenenergy $k_\nu^2/2$, where $\vec{k}_\nu$ is the asymptotic velocity of the ejected electron relative to B, and $\vec{v}$ is the impact velocity.

Equation (2.8) becomes

$$t_{n0}^{BA}=\int_{-\infty}^{\infty}dt(u_{n0}^{BA}-s_{n0}^{BA}u_{00}^{AA}) \times\exp\left[i\int_{-\infty}^{t}(\omega_n^B-\omega_0^A+u_{nn}^{BB}-u_{00}^{AA})dt\right] \quad (3.2a)$$

for charge transfer,

$$t_{n0}^{AA}=\int_{-\infty}^{\infty}dt\,u_{n0}^{AA} \times\exp\left[i\int_{-\infty}^{t}(\omega_n^A-\omega_0^A+u_{nn}^{AA}-u_{00}^{AA})dt\right] \quad (3.2b)$$

for excitation, and

$$t_{\nu 0}^{BA}=\int_{-\infty}^{\infty}dt(u_{\nu 0}^{BA}-s_{\nu 0}^{BA}u_{00}^{AA}) \times\exp\left[i\int_{-\infty}^{t}(\tfrac{1}{2}k_\nu^2-\omega_0^A+u_{\nu\nu}^{BB}-u_{00}^{AA})dt\right] \quad (3.2c)$$

for ionization, where

$$s_{ij}^{BA}=[\xi_i^B,\xi_j^A]\,, \tag{3.3a}$$

$$u_{ij}^{BA}=\left[\xi_i^B,\left[-\frac{Z_B}{r_B}\right]\xi_j^A\right]\,, \tag{3.3b}$$

$$u_{ij}^{BB}=\left[\xi_i^B,\left[-\frac{Z_A}{r_A}\right]\xi_j^B\right]\,, \tag{3.3c}$$

and

$$u_{ij}^{AA}=\left[\xi_i^A,\left[-\frac{Z_B}{r_B}\right]\xi_j^A\right]\,. \tag{3.3d}$$

In Eq. (3.2c), we have $u_{vv}^{BB}=0$, since Coulomb wave functions centered on B given by Eq. (3.1c) are used for the continuum states.

The method of numerical calculations of Eq. (3.2a) has been described previously,[8] and the same method was applied to calculations of Eq. (3.2b). Numerical calculations of Eq. (3.2c) were performed as described in the following.

In the spherical coordinates centered on B with polar axis in the direction of impact of B, we will express $\vec{r}_B=(r_B,\theta_B,\psi_B)$, $\vec{k}_v=(k,\theta,\psi)$, $\vec{v}=(v,0,0)$, and $-\vec{R}=(R,\delta,0)$, where $\vec{R}$ is the position vector of B relative to A. The momentum-transfer factor $\exp(-i\vec{v}\cdot\vec{r})$, Coulomb wave function $\psi_v^B(\vec{r}_B)$, and ground-state wave function of the hydrogenlike atom $\phi_0^A(\vec{r}_A)$, which is the initial state here, are expanded as

$$\exp(-i\vec{v}\cdot\vec{r})=e^{-i\vec{v}\cdot\vec{R}/2}\sum_{\lambda=0}^{\infty}(-i)^{\lambda}(2\lambda+1)j_{\lambda}(vr_B)P_{\lambda}(\cos\theta_B)\,, \tag{3.4}$$

$$\psi_v^B(\vec{r}_b)=\sum_{l=0}^{\infty}(2l+1)i^l\exp(i\eta_l)\frac{f_l(r_B)}{kr_B}P_l(\cos\alpha)\,, \tag{3.5}$$

and

$$\begin{aligned}\phi_0^A(\vec{r}_A)&=\pi^{-1/2}Z_A^{3/2}e^{-Z_Ar_A}\\&=\pi^{-1/2}Z_A^{3/2}\sum_{n=0}^{\infty}C_n(r_B,R)P_n(\cos\beta)\,,\end{aligned} \tag{3.6}$$

where

$$f_l(r_B)\sim\sin\left[kr_B-\tfrac{1}{2}l\pi+\frac{Z_B}{k}\ln(2kr_B)+\eta_B\right]\quad(r_B\to\infty) \tag{3.7}$$

$$\eta_l=\arg\Gamma\left[1+l-i\frac{Z_A}{k}\right]\,, \tag{3.8}$$

$$\begin{aligned}C_n(r_B,R)=-(Rr_B)^{-1/2}\Bigg[&RI_{n+3/2}(Z_AR)K_{n+1/2}(Z_Ar_B)-r_BI_{n+1/2}(Z_AR)K_{n+3/2}(Z_Ar_B)\\&+\frac{2n+1}{Z_A}I_{n+1/2}(Z_AR)K_{n+1/2}(Z_Ar_B)\Bigg]\,,\end{aligned} \tag{3.9}$$

$$\cos\alpha=\cos\theta\cos\theta_B+\sin\theta\sin\theta_B\cos(\psi-\psi_B)\,, \tag{3.10}$$

$$\cos\beta=\cos\delta\cos\theta_B+\sin\delta\sin\theta_B\cos\psi_B\,, \tag{3.11}$$

and $P_l(x)$ is the Legendre function, $j_\lambda(x)$ the spherical Bessel function, $\Gamma(z)$ the gamma function, and $I_n(x)$ and $K_n(x)$ are the modified Bassel functions. The coefficients $\{f_l(r_B)\}$ can be obtained with the computer code developed by Barnett *et al.*[25] The Legendre functions $P_l(\cos\alpha)$ and $P_n(\cos\beta)$ can be rewritten as follows:

$$P_l(\cos\alpha)=P_l(\cos\theta)P_l(\cos\theta_B)+2\sum_{m=1}^{l}\frac{(l-m)!}{(l+m)!}P_l^m(\cos\theta)P_l^m(\cos\theta_B)\cos m(\psi-\psi_B) \tag{3.12}$$

and

$$P_n(\cos\beta)=P_n(\cos\delta)P_n(\cos\theta_B)+2\sum_{\mu=1}^{n}\frac{(n-\mu)!}{(n+\mu)!}P_n^{\mu}(\cos\delta)P_n^{\mu}(\cos\theta_B)\cos\mu\psi_B\ , \tag{3.13}$$

where P_l^m is the associate Legendre function. Using Eqs. (3.12) and (3.13) in Eqs. (3.5) and (3.6), and then inserting Eqs. (3.4)—(3.6) into Eqs. (3.3a) and (3.3b), we perform integration with respect to (θ_B,ψ_b), where we use

$$P_\lambda(\cos\theta_B)P_n^m(\cos\theta_B)=\sum_{\eta=m}^{\lambda+n}Q(\lambda,n,m,\eta)P_\eta^m(\cos\theta_B)\ . \tag{3.14}$$

The coefficient $Q(\lambda,n,m,\eta)$ can be easily obtained. Using Eqs. (3.3a) and (3.3b) in Eq. (3.2c), we get

$$t_{\nu 0}^{BA}=\sum_{l=0}^{\infty}\sum_{m=0}^{l}B_{klm}(\rho)D_{lm}^{-1/2}P_l^m(\cos\theta)\cos m\psi\ , \tag{3.15}$$

where

$$D_{lm}=\frac{2\pi(l+m)!}{(2l+1)(l-m)!}(1+\delta_{m0})\ , \tag{3.16}$$

$$B_{klm}(\rho)=\int_{-\infty}^{\infty}dt\exp\left[i\int_{-\infty}^{t}(\tfrac{1}{2}k^2-\omega_0-\tfrac{1}{2}v^2-U_{00}^{AA})dt\right]E_{klm}\ , \tag{3.17}$$

$$E_{klm}=D_{lm}^{1/2}\sum_{n=0}^{\infty}\sum_{\lambda=0}^{\infty}F_{lmn\lambda}(\cos\delta)G_{kln\lambda}(R)\ , \tag{3.18}$$

$$F_{lmn\lambda}(\cos\delta)=8\pi^{1/2}Z_A^{3/2}\frac{(-i)^{l+\lambda}(2\lambda+1)(n-m)!Q(\lambda,n,m,l)}{(n+m)!(1+\delta_{m0})}\exp(-i\eta_l)P_l^m(\cos\delta)\ , \tag{3.19}$$

$$G_{kln\lambda}(R)=-\int_0^{\infty}\frac{f_l(r_B)}{kr_B}\left[\frac{Z_B}{r_B}+u_{00}^{AA}\right]C_n(r_B,R)\times j_\lambda(vr_B)r_B^2dr_B\ , \tag{3.20}$$

and

$$u_{00}^{AA}=-\frac{Z_B}{R}[1-(1+Z_AR)e^{-2Z_AR}]\ , \tag{3.21}$$

where $\vec{v}\cdot\vec{R}=v^2t$ and $\delta_{m0}=1$ for $m=0$ and $\delta_{m0}=0$ for $m\neq 0$. The DWBA cross section for ionization is given by

$$\sigma_{\rm ion}^{\rm DWBA}=2\pi\int_0^{\infty}p_{\rm ion}(\rho)\rho\,d\rho\ , \tag{3.22}$$

where

$$p_{\rm ion}(\rho)=\int_0^{\infty}dk\sum_{l=0}^{\infty}\sum_{m=0}^{l}p_{klm}(\rho) \tag{3.23}$$

and

$$p_{klm}(\rho)=\frac{k^2}{8\pi^3}|B_{klm}(\rho)|^2\ . \tag{3.24}$$

The doubly differential UDWA cross section is given by

$$\frac{d\sigma}{d\Omega\,d\epsilon}=\frac{k}{4\pi^2}\sum_{m=0}^{\infty}\frac{1+\delta_{m0}}{2}\int_0^{\infty}\rho\,d\rho\left|\sum_{l=m}^{\infty}B_{klm}(\rho)D_{lm}^{-1/2}P_l^m(\cos\theta)\right|^2p^{-1}\sin^2p^{1/2} \tag{3.25}$$

in the system moving with velocity $\vec{v}$, where $\epsilon=\frac{1}{2}k^2$ and

$$p=p_{\rm ion}+p_{\rm exci}+p_{CT}\ , \tag{3.26}$$

where $p_{\rm ion}$ is given by Eq. (3.23) and

$$p_{\rm exci}=\sum_{n\neq 0}|t_{n0}^{AA}|^2 \tag{3.27}$$

and

$$P_{CT}=\sum_n|t_{n0}^{BA}|^2\ . \tag{3.28}$$

The upper limit of l was enough to be set as $l_{\max}=30$ for impact energies below 200 keV/amu, however, it needed $l_{\max}>50$ for impact energies above 500 keV/amu. In this work, calculations of Eq. (3.17) were performed for l up to $L\simeq 50$, and then $B_{klm}(\rho)$ was modified to account the contribution from range $L<l<l_{\max}(\simeq 100)$ as described below. First, DWBA cross sections were determined for $l\leq L$.

$$\sigma_{kl}^{\mathrm{DWBA}}=2\pi\int_0^\infty p_{kl}(\rho)\rho\, d\rho\ , \tag{3.29}$$

with

$$p_{kl}(\rho)=\sum_{m=0}^{l} p_{klm}(\rho)\ . \tag{3.30}$$

Then, for $l>L$, DWBA cross sections were evaluated by extrapolation, and $p_{kl}(\rho)$ was determined as follows:

$$p_{kl}(\rho)=\frac{\sigma_{kl}^{\mathrm{DWBA}}}{\sigma_{kL}^{\mathrm{DWBA}}}p_{kL}(L\rho/l)\quad (l>L)\ . \tag{3.31}$$

Finally, $B_{klm}(\rho)$ was modified as

$$\bar{B}_{klm}(\rho)=B_{klm}(\rho)R(\rho)\ , \tag{3.32}$$

with

$$R(\rho)=\left[\sum_{l=0}^{l_{\max}} p_{kl}(\rho)\right]^{1/2}\Big/\left[\sum_{l=0}^{L} p_{kl}(\rho)\right]^{1/2}\ . \tag{3.33}$$

In this work we use Coulomb wave functions centered on the projectile as $\psi_\nu^B(\vec{r}_B)$ in Eq. (3.1c). When the projectile charge is much greater than the charge of the target nucleus, that is, $Z_B>>Z_A$, this approach is adequate to evaluate ionization cross sections. Otherwise, it is necessary to modify this approach to include the effect of distortion of the wave function $\psi_\nu^B(\vec{r}_B)$, due to the potential around the target nucleus. The modification was made according to the following idea: At higher energies, charge transfer to the continuum makes little contribution to total ionization cross sections, where the total cross sections mainly result from low-energy distributions of ejected electrons due to glancing collisions. Therefore, the calculations with Coulomb wave functions centered on the target give more reasonable total cross sections than those with the wave functions centered on the projectile. It is probable that the present treatment with Coulomb wave functions centered on the projectile overestimates ionization cross sections for lower values of projectile charge. Actually, numerical calculations of DWBA cross sections for the impact of H^+ on H showed that the results with the wave function centered on the projectile were about 70% larger than those with the wave function centered on the target at the proton-impact energies 10—1000 keV. This implies that the distortion of the final-state wave function due to the electron-target-nucleus interaction reduces the DWBA cross section by about 40%. This fact enables us to approximately take into account the effect of the distortion:

$$\sigma_{\mathrm{ion,AB}}^{\mathrm{DWBA}}(E)=D\sigma_{\mathrm{ion,B}}^{\mathrm{DWBA}}(E) \tag{3.34}$$

with

$$D=\lim_{E\to\infty}\sigma_{\mathrm{ion,A}}^{\mathrm{DWBA}}(E)/\sigma_{\mathrm{ion,B}}^{\mathrm{DWBA}}(E)\ , \tag{3.35}$$

where E is the impact energy, $\sigma_{\mathrm{ion,AB}}^{\mathrm{DWBA}}(E)$ the DWBA cross section with inclusion of the distortion of the final-state wave function due to the potentials of A (projectile) and B (target nucleus), and $\sigma_{\mathrm{ion,A}}^{\mathrm{DWBA}}(E)$ and $\sigma_{\mathrm{ion,B}}^{\mathrm{DWBA}}(E)$ are the DWBA cross sections with the Coulomb wave function centered on A and B, respectively. Numerical calculations showed that $D=0.591$, 0.724, and 1 for impacts of H^+, C^{6+}, and Si^{14+} on H.

The DWBA transition matrix $t_{\nu 0}^{BA}$ given by Eq. (3.2c) was renormalized corresponding to Eq. (3.34) as

$$t_{\nu 0}^{BA}\to D^{1/2}t_{\nu 0}^{BA}\ , \tag{3.36}$$

where we used $D=0.591$, 0.669, 0.709, 0.724, and 1 for impacts of H^+, Li^{3+}, B^{5+}, C^{6+}, and Si^{14+} on H. The second and third values of D were obtained by interpolation.

IV. RESULTS AND DISCUSSION

A. Ionization

The doubly differential cross section $d^2\sigma/d\epsilon\, d\Omega$ in the laboratory system for ionization in the collision of protons with atomic hydrogen at the energy of 300 keV/amu is shown in Fig. 1, and compared with the results obtained by Macek,[21] Garibotti and Miraglia,[26] and with the experimental results of Rudd[20] which were confirmed by Toburen and Wilson.[27] The results of Macek and Rudd are for molecular hydrogen targets. The figures show their values divided by two.

Macek used the first term in the Neumann expansion of Faddeev's equation for the final state of

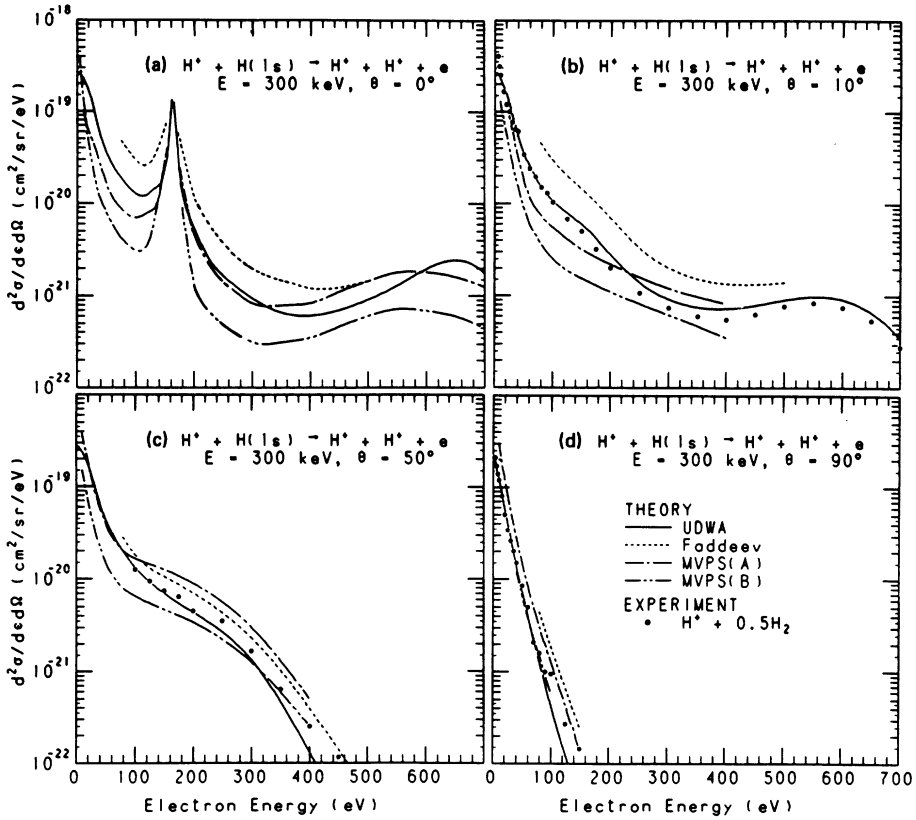

FIG. 1. Doubly differential cross sections for electrons ejected at various angles as a function of ejected energy for 300-keV proton impact on atomic hydrogen. UDWA denotes the present results; Faddeev, the results of Macek using Faddeev's equation (Ref. 21); and MVPS, the results of Garibotti and Miraglia using a modified Vainshtein-Presnyakov-Sobelman method. (a) Without and (b) with the internuclear interaction (Ref. 26). The solid circles show half the value of experimental cross sections obtained by Rudd for proton impact on molecular hydrogen (Ref. 20).

the electron-proton-residual ion system, where hydrogenic wave functions with an effective charge Z_{eff} equal to $(2I)^{1/2}$ (I is the ionization potential of H_2) are used for the system consisting of the electron and residual ion. His results show the same energy dependence as the present results. However, the former are higher than the latter at the smaller angles. This may be caused by the neglect of the nonorthogonality of initial- and final-state wave functions rather than the use of the effective charge Z_{eff}.

Garibotti and Miraglia use a final-state wave function which is the product of Coulomb waves. Their treatment is considered an improvement of the Vainshtein-Presnyakov-Sobelman method.[28] They consider two treatments: one includes the internuclear interaction and the other does not. As shown in Fig. 1, the results with the internuclear interaction are lower than those without. Their results follow the experimental values at the larger angles, but show a different energy dependence from that of the experiment at the smaller angles.

The present results fall into an underestimation at the larger angles and larger energies. This comes from the cutoff of the Legendre expansion series of the final-state wave functions used in this treatment.

The total ionization cross sections for the impact of protons on atomic hydrogen are shown in Fig. 2, compared with the results obtained with typical theories, and with experimental results of Fite *et al.*,[17] Gilbody and Ireland,[18] and Park *et al.*[19] Park *et al.* have normalized their data to the Born 2*s*-excitation cross section. The other data have been obtained by absolute measurements. All theoretical results shown tend toward the results of Bates and Griffing[16] based on the Born approximation. The calculations of Janev and Presnyakov[22] using a dipole-approximation close-coupling method with inclusion of transitions via the 2*p*-resonant state excellently agree with the experiments. Olson and Salop[7] have obtained the cross sections with the

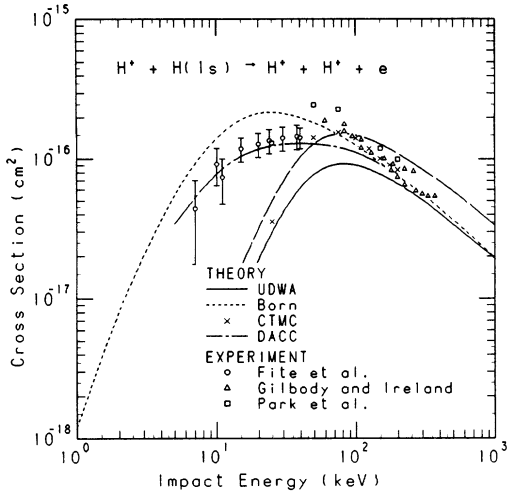

FIG. 2. Ionization cross sections for proton impact on atomic hydrogen. UDWA shows the present results, Born the results of Bates and Griffing based on Born approximation (Ref. 16), CTMC the results of Olson and Salop with classical-trajectory Monte Carlo method (Ref. 7), and DACC the results of Janev and Presnyakov with a dipole-approximation close-coupling method (Ref. 22). The circles, triangles, and squares are the experimental cross sections obtained by Fite *et al.* (Ref. 17), Gilbody and Ireland (Ref. 18), and Park *et al.* (Ref. 19), respectively. The long-dash curve shows the UDWA results without the renormalization given by Eq. (3.36).

classical-trajectory Monte Carlo method, which nearly follows Abrines's and Percival's results,[29] and which agree very well with Gilbody's and Ireland's data. However, those rapidly decrease with the decreasing energy below 60 keV/amu as in the present work. Both theories correctly include the charge transfer to the continuum. The rapid decreasing energy dependence suggests that the classical-trajectory Monte Carlo method probably ignores the ionizations via intermediate excited states or molecular states as in the present theory, while Rudd[30] and Janev and Presnyakov[22] consider the importance of these processes.

Total ionization cross sections are shown in Figs. 3 and 4 for the impact of C^{6+} and Si^{14+} ions, respectively, on atomic hydrogen. For comparison, other theoretical results are also shown: Born approximation, the classical-trajectory Monte Carlo method by Salop and Olson,[3] and Salop and Eichler,[31] sudden approximation by Salop and Eichler,[31] and the dipole-approximation close-coupling method by Janev and Presnyakov[22], in Fig. 3. Figure 4 includes the results with the Born

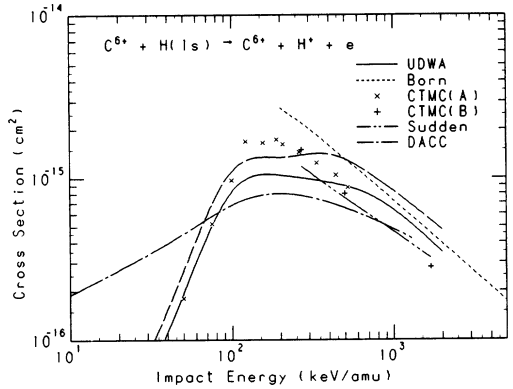

FIG. 3. Ionization cross sections for C^{6+} impact on atomic hydrogen. Notations are the same as those described in Fig. 2 except that CTMC(A) are the results of Salop and Olson (Ref. 3), CTMC(B) the results of Salop and Eichler (Ref. 31), and Sudden the results of Salop and Eichler using sudden approximation (Ref. 31).

approximation, the classical-trajectory Monte Carlo method by Olson and Salop,[7] and the dipole-approximation close-coupling method by Janev and Presnyakov.[22] The figure also includes the experimental cross sections divided by two for the impact of Fe^{14+} ions on molecular hydrogen by Berkner *et al.*[32,33] The theoretical results show different energy dependences. It is important to do further studies on this problem.

The ionization cross sections calculated with the UDWA method are all given in Fig. 5 and Table I. Figure 5 also shows the experimental cross sections divided by two for the impact of Li^{3+} ions on

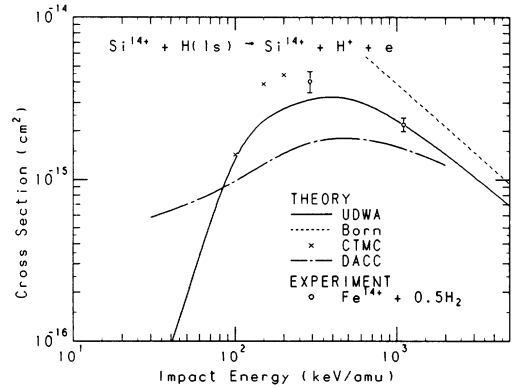

FIG. 4. Ionization cross sections for Si^{14+} impact on atomic hydrogen. Notations are the same as those described in Fig. 2. For comparison, the experimental cross sections obtained by Berkner *et al.* for Fe^{14+} impact on molecular hydrogen which are divided by two (Refs. 32 and 33) are also shown.

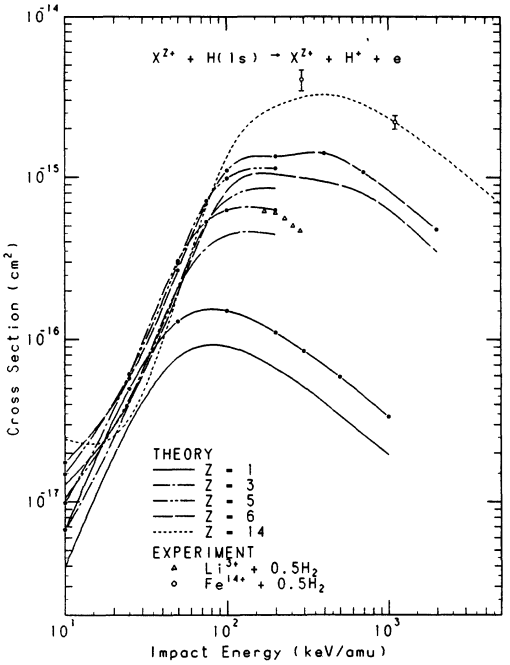

FIG. 5. Comparison of energy dependences of the ionization cross sections obtained in the present work for impacts of fully stripped ions having different charges on atomic hydrogen. Also shown are the experimental cross sections of Pivovar *et al.* for Li^{3+} impact on molecular hydrogen (Ref. 34) and Berkner *et al.* for Fe^{14+} impact on molecular hydrogen (Refs. 32 and 33). The lines with solid circles denote the UDWA results without the renormalization given by Eq. (3.36).

molecular hydrogen by Pivovar *et al.*[34]

Figure 6 shows the dependence of UDWA cross sections on projectile charge at the impact energy 1100 keV/amu, compared with the classical-trajectory Monte Carlo method by Berkner *et al.*,[32] the dipole-approximation close-coupling calculations by Janev and Presnyakov,[22] and experimental results by Berkner *et al.*[32] All results denote $Z^{1.82}$ dependence except the results of Janev and Presnyakov for $Z > 10$.

In Figs. 2, 3, and 5, the UDWA results without renormalization given by Eq. (3.36), are also shown. These overestimate the ionization cross sections at higher energies due to the neglect of distortion of the final-state wave function caused by the potential of the target nucleus.

The rapid decrease with decreasing impact energy below the energy at which the cross section denotes maximum, as shown in Figs. 2–5, more or less underestimates the ionization cross sections. This is attributed to the neglect of off-diagonal matrix elements except those involving the initial state which results in the neglect of transitions via some other intermediate states.

B. Excitation

The total excitation cross sections calculated with the UDWA method are shown in Fig. 7 and Table II. Figure 7 gives the results of Janev and

TABLE I. UDWA cross sections (cm^2) for ionization in $H^+ + H$, $Li^{3+} + H$, $B^{5+} + H$, $C^{6+} + H$, and $Si^{14+} + H$ collisions.

Impact energy (keV/amu)	H^+	Li^{3+}	B^{5+}	C^{6+}	Si^{14+}
5000					6.88(−16)[a]
2000				3.46(−16)	1.44(−15)
1000	1.94(−17)				2.32(−15)
700				7.89(−16)	
500	3.39(−17)				3.17(−15)
400				9.36(−16)	
300	5.08(−17)				
200	6.62(−17)	4.42(−16)	8.52(−16)	1.04(−15)	2.74(−15)
100	9.05(−17)	4.37(−16)	7.23(−16)	8.22(−16)	1.34(−15)
75		3.66(−16)	5.18(−16)		
50	7.72(−17)	2.07(−16)	2.10(−16)	1.94(−16)	1.89(−16)
25		4.06(−17)	4.34(−17)	4.16(−17)	3.27(−17)
10	3.96(−18)	6.57(−18)	1.05(−17)	1.27(−17)	2.44(−17)

[a] 6.88(−16) denotes 6.88×10^{-16}.

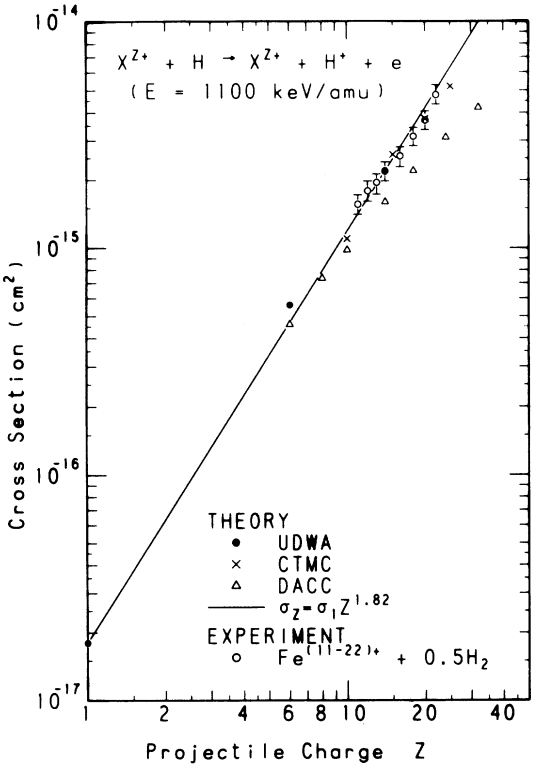

FIG. 6. Charge dependence of ionization cross sections for impacts of fully stripped ions on atomic hydrogen at 1100 keV/ amu. Notations have the same meanings as those described in Fig. 2. For comparison, the experimental cross sections of Berkner *et al.* for the impacts of Fe ions on molecular hydrogen (Ref. 32) are also shown.

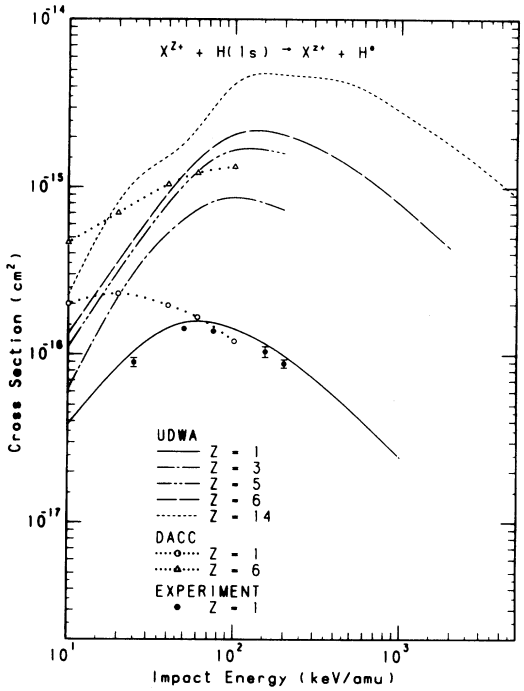

FIG. 7. Total excitation cross sections for impacts of fully stripped ions having different values of charge on atomic hydrogen. UDWA denotes the present results; DACC, the results of Janev and Presnyakov by dipole-approximation close-coupling calculations for excitation up to $n=5$ (Ref. 22), and the solid circles are the experimental results of Park *et al.* for excitation up to $n=4$ (Ref. 35).

TABLE II. UDWA cross sections (cm^2) for excitation in $H^+ + H$, $Li^{3+} + H$, $B^{5+} + H$, $C^{6+} + H$, and $Si^{14+} + H$ collisions.

Impact energy (keV/amu)	H^+	Li^{3+}	B^{5+}	C^{6+}	Si^{14+}
5000					8.86(−16)
2000				4.31(−16)	1.81(−15)
1000	2.43(−17)				2.86(−15)
700				1.05(−15)	
500	4.67(−17)				4.16(−15)
400				1.52(−15)	
300	7.25(−17)				
200	9.83(−17)	7.32(−16)	1.60(−15)	2.07(−15)	4.70(−15)
100	1.42(−16)	8.69(−16)	1.68(−15)	2.09(−15)	4.19(−15)
75		8.25(−16)	1.49(−15)		
50	1.55(−16)	6.46(−16)	1.04(−15)	1.21(−15)	1.86(−15)
25		3.08(−16)	4.29(−16)	4.90(−16)	1.08(−15)
10	3.83(−17)	6.17(−17)	1.10(−16)	1.32(−16)	2.26(−16)

Presnyakov with the dipole-approximation close-coupling method[22] for comparison. As seen from the figure the results of Janev and Presnyakov show quite a different energy dependence from the present results and denote four to five times larger values than these at the energy of 10 keV/amu.

Park *et al.*[35] have measured the energy dependence of cross sections for excitation of atomic hydrogen to the $n=2$, 3, and 4 states by protons. Absolute cross sections have been determined by normalization to the theoretical cross section through the use of Born approximation at the proton energy of 200 keV. As shown in the figure, their total cross sections agree with the present results at proton energies above 50 keV/amu. Detailed comparisons between theories based on different methods and experiments are described in Refs. 36–38 for excitation of atomic hydrogen to the $2s$ and $2p$ states by protons. It is known from these papers that below 10 keV, transition via some intermediate states are dominant. Therefore, UDWA theory cannot be applied below 10 keV.

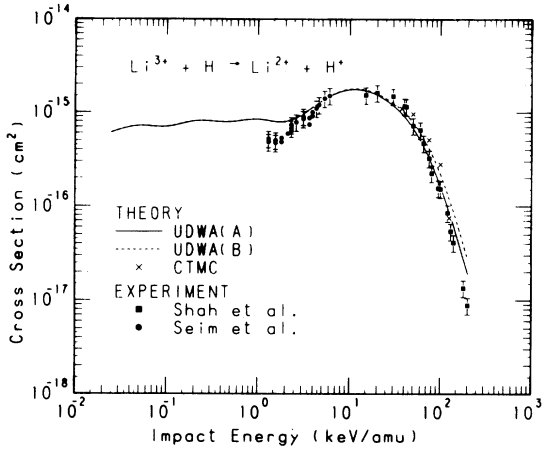

FIG. 8. Charge-transfer cross sections for Li^{3+} impact on atomic hydrogen. UDWA (A) denotes the present results; UDWA (B), the previous UDWA results without ionization and excitation channels (Ref. 9); CTMC, the results of Olson and Salop by classical-trajectory Monte Carlo calculations (Ref. 7); solid squares, the experimental results of Shah *et al.* (Ref. 39); and solid circles, those of Seim *et al.* (Ref. 13).

C. Charge transfer

The present results of charge-transfer cross sections for impacts of Li^{3+}, B^{5+}, C^{6+}, and Si^{14+} ions on atomic hydrogen are shown in Figs. 8–11, compared with the classical-trajectory Monte Carlo calculations by Olson and Salop[7] and experiments. The experimental cross sections shown in the figures are by Shah *et al.*[39] and Seim *et al.*[13] for the impact of Li^{3+} ions, Goffe *et al.*[12] for the impacts of B^{5+} and C^{6+} ions, and Crandall *et al.*[40] for the impact of B^{5+} ions, and Meyer *et al.*[41] for the impacts of Fe^{14+}, Mo^{14+}, Ta^{14+}, Au^{14+}, and W^{14+} ions. Berkner *et al.*[32] have measured charge-transfer cross sections for the impacts of Fe ions including Fe^{14+} on molecular hydrogen. The data for the impact of Fe^{14+} divided by two are shown in Fig. 11. All numerical results of the present work are shown in Table III.

The UDWA results agree quite well with the experiments except at the higher and lower energies in the $Li^{3+} + H$ case. The figures also include UDWA results with neglect of the ionization and excitation channels.[9,10] The comparison with the present results shows an importance of the inclusion of ionization and excitation channels even at the energies of MeV range.

It is interesting to see the energy dependence of UDWA cross sections shown in Fig. 11. The curve denoting the results with inclusion of ionization and excitation channels most deviates from that without those channels at the energies from 100 to 2000 keV/amu and the discrepancy becomes smaller with increasing energy above 2000 keV/amu. In consequence, the curve is concave in the vicinity of 1000 keV/amu.

Figure 12 shows a scaling of the charge-transfer cross sections based on the UDWA cross sections

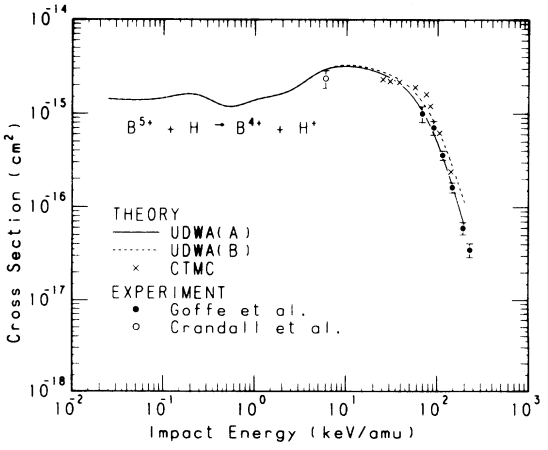

FIG. 9. Charge-transfer cross sections for B^{5+} impact on atomic hydrogen. Notations have the same meanings as those described in Fig. 8 except that the solid circles show the experimental results of Goffe *et al.* (Ref. 12) and open circles those of Crandall *et al.* (Ref. 40).

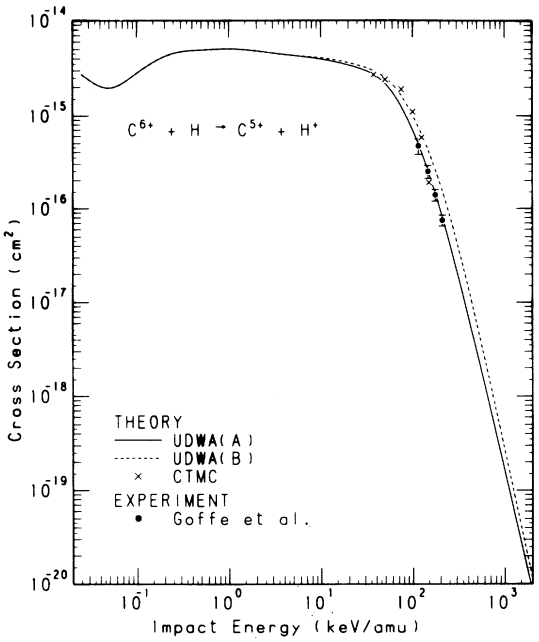

FIG. 10. Charge-transfer cross sections for C^{6+} impact on atomic hydrogen. Notations are the same as those described in Fig. 8.

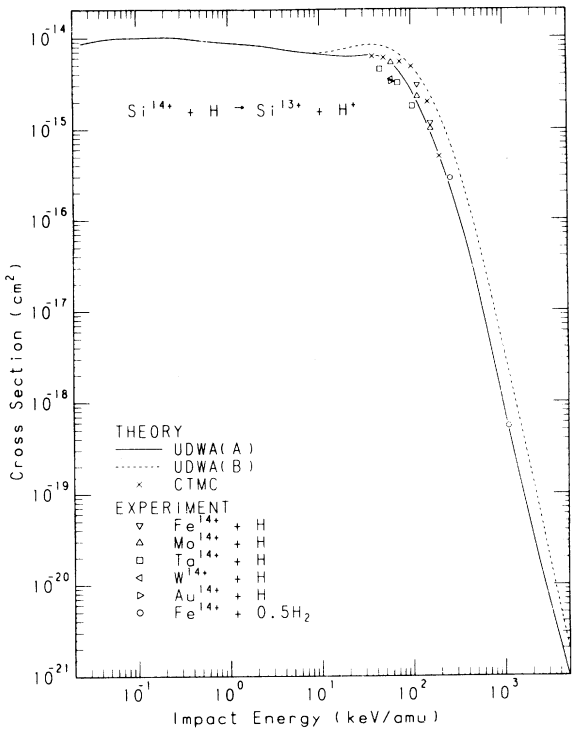

FIG. 11. Charge-transfer cross sections for Si^{14+} impact on atomic hydrogen. Notations are the same as those described in Fig. 8. For comparison, the experimental cross sections of Meyer *et al.* for impacts of Fe^{14+}, Mo^{14+}, Ta^{14+}, W^{14+}, and Au^{14+} ions on atomic hydrogen (Ref. 42) and those of Berkner *et al.* for impacts of Fe^{14+} ions on molecular hydrogen (Ref. 32) are also shown.

obtained in the present calculations, where the cross sections and collision energies are scaled by

$$\sigma(E)=\alpha\tilde{\sigma}(\tilde{E}) \tag{4.1}$$

and

$$E=\beta\tilde{E}\ , \tag{4.2}$$

with

$$\alpha=Z^{1.07} \tag{4.3}$$

and

$$\beta=Z^{0.350}\ , \tag{4.4}$$

where $\sigma(E)$ denotes the cross section at the energy of E, $\tilde{\sigma}(\tilde{E})$ is the scaled cross section with the scaled energy $\tilde{E}$, and Z is the charge of the projectile. The scaling factors α and β were determined so as to fit the Si^{14+} curve to the H^+ curve at the energies $\tilde{E}>10$ keV/amu, and to the Ca^{20+} points[10] at the energies $\tilde{E}<10$ keV/amu. The present results do not completely fit one another at the higher energies; this is different from previous work,[10] which did not use ionization and excitation channels.

The scaling procedure is also applied to experimental cross sections obtained by Gardner *et al.*,[41] Meyer *et al.*,[42] Berkner *et al.*,[32,43] and Crandall *et al.*[14] The results are shown in Fig. 13 with the scaled UDWA cross sections for $Si^{14+}+H$ and $Ca^{20+}+H$ collisions. Figure 13 shows the data of Berkner *et al.*, for molecular hydrogen targets, after being divided by two. All data shown in the figure are restricted to $Z\geq 12$. The scaled experimental cross sections successfully fall on the Si^{14+} curve. In particular, the agreement of the data of Berkner *et al.* for $Z=12-25$ with the Si^{14+} curve is quite perfect in the energy range $\tilde{E}=350-1200$ keV/amu, although the curve is concave there. From this fact and the fact that the UDWA results for the $Ca^{20+}+H$ collisions have been fitted to the Si^{14+} curve, it can be proposed to use the Si^{14+} curve as a "universal curve" to estimate the cross sections for high values of projectile charge. In the energy range $\tilde{E}=0.01-1$ keV/amu, this curve can be approximately expressed as (in units of cm^2)

$$\tilde{\sigma}(\tilde{E})=5.3\times 10^{-16}\ . \tag{4.5}$$

At low energies $E<10$ keV/amu, as described in

TABLE III. UDWA cross sections (cm^2) for charge transfer in $H^+ + H$, $Li^{3+} + H$, $B^{5+} + H$, $C^{6+} + H$, and $Si^{14+} + H$ collisions.

Impact energy (keV/amu)	H^+	Li^{3+}	B^{5+}	C^{6+}	Si^{14+}
5000					9.28(−22)
2000				8.18(−21)	3.73(−20)
1000	6.44(−22)				7.94(−19)
700				7.05(−19)	
500	2.20(−20)				2.03(−17)
400				6.94(−18)	
300	2.35(−19)				
200	1.29(−18)	1.90(−17)	6.20(−17)	9.34(−17)	5.00(−16)
100	1.54(−17)	1.63(−16)	4.87(−16)	6.92(−16)	2.62(−15)
75		3.25(−16)	9.02(−16)		
50	9.62(−17)	6.74(−16)	1.62(−15)	2.17(−15)	5.93(−15)
25	3.18(−16)	1.35(−15)	2.61(−15)	3.20(−15)	6.22(−15)
10	7.95(−16)	1.75(−15)	3.17(−15)	3.94(−15)	6.58(−15)
5		1.33(−15)	2.75(−15)	4.31(−15)	7.17(−15)
4	1.09(−15)				
2.5			1.78(−15)	4.68(−15)	8.06(−15)
2		7.96(−16)			
1	1.63(−15)	8.42(−16)	1.39(−15)	5.06(−15)	8.80(−15)
0.5		7.91(−16)	1.19(−15)	4.92(−15)	9.40(−15)
0.4	1.99(−15)				
0.25			1.55(−15)	4.54(−15)	1.01(−14)
0.2		8.05(−16)			
0.1	2.76(−15)	7.03(−16)	1.46(−15)	2.81(−15)	9.98(−15)
0.05		7.19(−16)	1.39(−15)	1.96(−15)	9.77(−15)
0.04	3.50(−15)				
0.025		6.09(−16)	1.43(−15)	2.73(−15)	8.65(−15)
0.01	3.72(−15)				

the Appendix, a classical-barrier theory[11] shows that a reasonable value of the cross sections is somewhere between σ_{up} and σ_{low}, where

$$\sigma_{up} \simeq 2[2(Z+1)^{1/2}+1]^2\sigma_0 \tag{4.6}$$

and

$$\sigma_{low} \simeq 2(Z-2)^2/\{(Z-1)^2/[\nu(Z-1)-1]^2-1\}^2\sigma_0 , \tag{4.7}$$

with

$$\sigma_0 = 8.8\times 10^{-17}\ (cm^2) \tag{4.8}$$

and

$$\nu(Z) = [(2Z^{1/2}+1)/(Z+2Z^{1/2})]^{1/2}Z , \tag{4.9}$$

where Z is the effective charge of the projectile. Figure 14 shows σ_{up} and σ_{low} with experimental cross sections reported in Ref. 14, and the UDWA cross sections for the collision energies $E \leq 10$ keV/amu.[8–10] Strictly speaking, we must use the effective charge of the projectile as Z for partially stripped ions. However, for practical convenience, we can use the charge of ions as Z. In the figure, it is seen that all data of Crandall *et al.* exist between the upper and lower limits defined by Eqs. (4.6) and (4.7).

Estimation of the upper limit of charge-transfer cross sections at low energies is important for the design and operation of controlled thermonuclear fusion devices. Figure 14 also shows the results of the electron-tunneling theory by Grozdanov and Janev[44] and the absorbing-sphere model calculations by Olson and Salop.[45] The recent work of Salop and Olson[15] for $Fe^{26+} + H$ collision system seems to support the electron-tunneling theory, while charge dependence of the UDWA cross sections at the higher charges are close to the

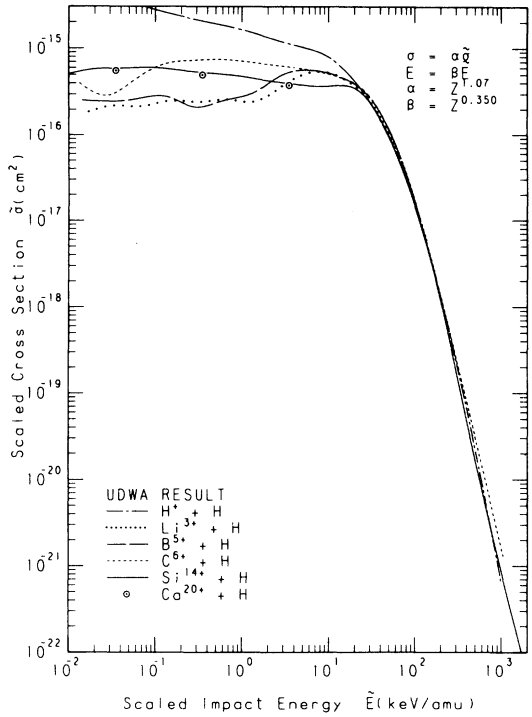

FIG. 12. Scaled UDWA charge-transfer cross sections $\tilde{\sigma}$ vs scaled impact energy $\tilde{E}$ where cross sections σ and impact energy E are given by $\sigma=\alpha\tilde{\sigma}$ and $E=\beta\tilde{E}$ with $\alpha=Z^{1.07}$ and $\beta=Z^{0.350}$. The cross sections for Ca^{20+} impact are taken from Ref. 10.

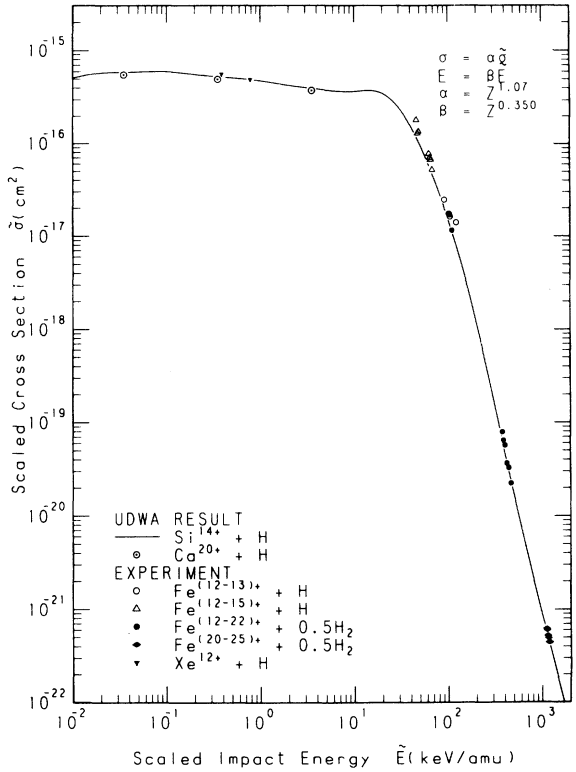

FIG. 13. Results of application of the scaling rule to experimental charge-transfer cross sections for impacts of highly stripped ions ($Z \geq 12$) on atomic and molecular hydrogen. Open circles denote the results of Gardner *et al.* (Ref. 41); open triangles, the results of Meyer *et al.* (Ref. 42); solid circles, the results of Berkner *et al.* (Ref. 32); diamonds, the results of Berkner *et al.* (Ref. 43); and solid triangles, the results of Crandall *et al.* (Ref. 14). Also shown, for comparison, are the UDWA results for impact of Si^{14+} and Ca^{20+} ions on atomic hydrogen. The Si^{14+} curve can be used as a universal curve to estimate charge-transfer cross sections for impact of highly stripped ions ($Z \geq 15$) on atomic hydrogen.

absorbing-sphere model calculations, rather than the electron-tunneling theory. However, the upper limit of the present theory agrees with these theories to within 50%.

Finally, we must note the recent work of Eichler.[46] Using eikonal theory he has calculated charge-transfer cross sections for a large number of collision systems including collisions of ions having charge $Z=1-10$, 15, 20, and 25 on H($1s$). Eichler's results show good agreement with experimental data, except that no energy-dependent curves of cross section for higher values of projectile charge show the concave curve at higher energies, while experimental data of Berkner *et al.*[32,43] clearly denote it as shown in Fig. 13. Comparison of the eikonal theory to the UDWA theory, has concluded that the overestimation of cross sections by a factor of about 3 in the previous UDWA results[8–10] may be largely attributed to the off-diagonal matrix elements ignored in the UDWA theory. Although his conclusion based on the Born series is true for the eikonal theory, it is not the case in the UDWA theory. The present work shows that the overestimation of cross sections for charge transfer in the previous work[8–10] is attributed to the neglect of excitation and ionization channels. The appearance of the concave curve in energy-dependence curves of cross sections at higher energies has been supported by the experiments of Berkner *et al.*[32,43], as shown in Fig. 13, which is nothing except the contribution of excitation and ionization channels.

V. CONCLUDING REMARKS

In the present paper, an attempt to perform UDWA calculations based on a complete set of

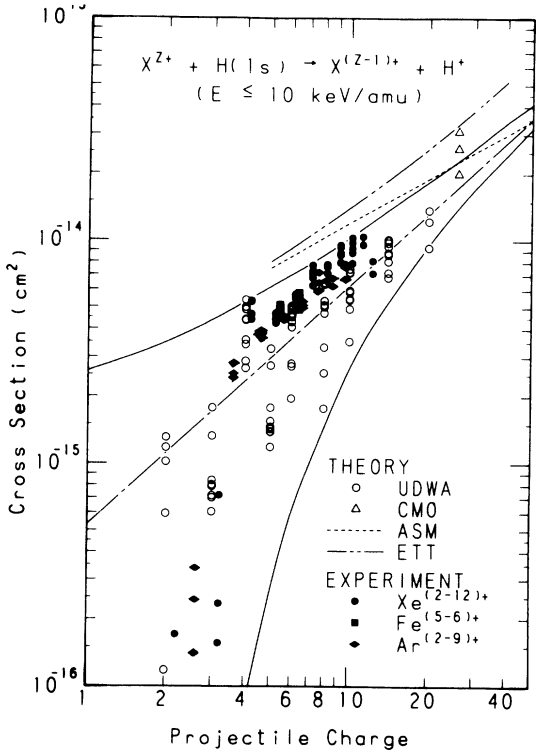

FIG. 14. Charge-transfer cross sections for impacts of different ions ($Z \geq 2$) on atomic hydrogen at low energies $E \leq 10$ keV/amu. UDWA denotes UDWA results for $E \leq 10$ keV/amu (Refs. 8–10); CMO, the results of Salop and Olson with the method of coupled molecular orbitals for Fe^{26+} impact at energies $E = 0.2$, 1.3, and 5.2 keV/amu which increase with impact energy (Ref. 15); ASM, absorbing-sphere-model calculations by Olson and Salop at $E = 2.5$ keV/amu (Ref. 45); ETT, electron-tunneling-theory calculations by Grozdanov and Janev at $E = 2.5$ keV/amu (Ref. 44); and experimental data are the results of Crandall *et al.* at the impact energies $E = 0.05-5$ keV/amu (Ref. 14), where the data of charge values being Z are plotted between Z and $Z+1$. The solid curves show the upper and lower limits estimated from the classical-barrier theory (Ref. 11) in combination with UDWA calculations. The dot-dashed straight line denotes the charge dependence given by $\sigma = 5.3 \times 10^{-16} Z^{1.07}$ (cm²) which corresponds to $\tilde{\sigma}(\tilde{E}) = 5.3 \times 10^{-16}$ (cm²): the average value of the solid curve shown in Fig. 13 for $\tilde{E} < 1$ keV/amu.

channels is described. The calculations have been applied to the collision systems involving atomic hydrogen and the incident fully stripped ions H^+, Li^{3+}, B^{5+}, C^{6+}, and Si^{14+}, which include the systems for which experimental charge-transfer cross sections are available to be compared with the obtained results, and which serve to derive a scaling rule to charge-transfer cross sections. The results show the following:

(i) The ionization cross sections denote the $Z^{1.82}$ dependence at the higher impact energies where Z is the projectile charge.

(ii) The charge-transfer cross sections for Li^{3+}, B^{5+}, and C^{6+} impacts show a perfect agreement with experimental data except for a few data points.

(iii) The inclusion of ionization and excitation channels considerably decreases charge-transfer cross sections at the impact energies $E > 100$ keV/amu for the higher values of projectile charge. In particular, in the case of Si^{14+} impact this effect is most pronounced in the vicinity of $E = 1000$ keV/amu and, consequently, the energy-dependence curve is concave there.

(iv) In the scaled frame, the above-stated energy-dependence curve almost completely fit the UDWA results for Ca^{20+} impacts and the experimental data for the range of projectile charge $Z = 14-25$. This fact suggests that the Si^{14+} curve can be used as a universal curve to estimate charge-transfer cross sections for high Z.

It is also known from the present calculations that the ionization cross sections for $H^+ + H$ collision system cannot be reproduced by the present UDWA method at the collision energies $E << 100$ keV. At these energies, transitions via charge-transfer channels and/or excitation channels are dominant as suggested by Rudd.[30] The UDWA method ignores such transitions in consequence of the neglect of off-diagonal transition matrix elements except those including the initial state.

The reasonable upper limit estimation of charge-transfer cross sections is important for the design and operation of controlled thermonuclear fusion devices. The present result agrees with other theories to within 50%.

ACKNOWLEDGMENTS

The author would like to express his thanks to Professor Tsutomu Watanabe for his continual encouragement and to Professor Takeshi Ishihara and Dr. Masao Sataka for their supportive discussions. Thanks are also due to Dr. R. K. Janev and Dr. L. P. Presnyakov for informing the author of their work prior to publication, to Mr. Minoru Maeda for providing the computer codes for this work, and to Miss Noriko Kanazawa for her continuous assistance in computation and the preparation of this paper.

APPENDIX

It is deduced from classical treatment[11] that at low energies, the cross sections oscillate as a function of the effective charge of projectile, which is received by the transferred electron. The envelope connecting the peaks is given by

$$\sigma_{\rm up} \simeq \tfrac{1}{2}\pi R_{\rm max}^2 , \tag{A1}$$

with

$$R_{\rm max} = 2(Z-1)/(Z^2/n_p^2 - 1) , \tag{A2}$$

and that connecting the ballay is given by

$$\sigma_{\rm low} \simeq \tfrac{1}{2}\pi R_{\rm min}^2 , \tag{A3}$$

with

$$R_{\rm min} = 2(Z-1)/[Z^2/(n_p-1)^2 - 1] , \tag{A4}$$

where

$$n_p = [(2Z^{1/2}+1)/(Z+2Z^{1/2})]^{1/2} Z \tag{A5}$$

and Z is the effective charge. These can be rewritten as

$$\sigma_{\rm up} \simeq 2\pi(2Z^{1/2}+1)^2 \tag{A6}$$

and

$$\sigma_{\rm low} \simeq 2\pi(Z-1)^2/[Z^2/(n_p-1)^2 - 1]^2 . \tag{A7}$$

Equations (A6) and (A7) denote the upper and lower limits, respectively, of the cross sections for a given value of the effective charge Z.

The UDWA calculations show that if we replace Z in Eq. (A6) by $Z+1$ and Z in Eqs. (A5) and (A7) by $Z-1$, we can use these equations for collision energies below 10 keV. Therefore, we will rewrite Eqs. (A5)–(A7) as

$$\sigma_{\rm up} \simeq 2\pi[2(Z+1)^{1/2}+1]^2 \tag{A8}$$

and

$$\sigma_{\rm low} \simeq 2\pi(Z-2)^2/\{(Z-1)^2/[\nu(Z-1)-1]^2 - 1\}^2 , \tag{A9}$$

with

$$\nu(Z) = [(2Z^{1/2}+1)/(Z+2Z^{1/2})]^{1/2} Z . \tag{A10}$$

[1] R. E. Olson, *Electronic and Atomic Collisions*, edited by N. Oda and K. Takayanagi (North-Holland, Amsterdam, 1980), p. 391.
[2] R. K. Janev and L. P. Presnyakov, Phys. Rep. 70, 1 (1981).
[3] A. Salop and R. E. Olson, Phys. Rev. A 16, 1811 (1977).
[4] A. Salop and R. E. Olson, Phys. Rev. A 19, 1921 (1979).
[5] J. Vaaben and J. S. Briggs, J. Phys. B 10, L521 (1977).
[6] C. Harel and A. Salin, J. Phys. B 10, 3511 (1977).
[7] R. E. Olson and A. Salop, Phys. Rev. A 16, 531 (1977).
[8] H. Ryufuku and T. Watanabe, Phys. Rev. A 18, 2005 (1978).
[9] H. Ryufuku and T. Watanabe, Phys. Rev. A 19, 1538 (1979).
[10] H. Ryufuku and T. Watanabe, Phys. Rev. A 20, 1828 (1979).
[11] H. Ryufuku, K. Sasaki, and T. Watanabe, Phys. Rev. A 21, 745 (1980).
[12] T. V. Goffe, M. B. Shah, and H. B. Gilbody, J. Phys. B 12, 3763 (1979).
[13] W. Seim, A. Müller, and E. Salzborn, Phys. Lett. 80A, 20 (1980).
[14] D. H. Crandall, R. A. Phaneuf, and F. W. Meyer, Phys. Rev. A 22, 379 (1980).
[15] A. Salop and R. E. Olson, Phys. Lett. 71A, 407 (1979).
[16] D. R. Bates and G. W. Griffing, Proc. Phys. Soc. London, Sect. A 66, 961 (1953).
[17] W. L. Fite, R. F. Stebbings, D. G. Hummer, and R. T. Brackmann, Phys. Rev. 119, 663 (1960).
[18] H. B. Gilbody and J. V. Ireland, Proc. R. Soc. London, Sect. A 277, 137 (1964).
[19] J. T. Park, J. E. Aldag, J. M. George, J. L. Peacher, and J. H. McGuire, Phys. Rev. A 15, 508 (1977).
[20] M. E. Rudd, C. A. Sautter, and C. L. Bailey, Phys. Rev. 151, 20 (1966).
[21] J. Macek, Phys. Rev. A 1, 235 (1970).
[22] R. K. Janev and L. P. Presnyakov, J. Phys. B 13, 4233 (1980).
[23] D. R. Bates, Proc. R. Soc. London, Sect. A 247, 294 (1958).
[24] R. Shakeshaft and L. Spruch, Rev. Mod. Phys. 51, 369 (1979).
[25] A. R. Barnett, D. H. Feng, J. W. Steed, and L. J. B. Goldfarb, Comp. Phys. Commun. 8, 377 (1974); A. R. Barnett, *ibid.* 11, 141 (1976).
[26] C. R. Garibotti and J. E. Miraglia, Phys. Rev. A 21, 572 (1980).
[27] L. H. Toburen and W. E. Wilson, Phys. Rev. A 5, 247 (1972).

[28]L. Vainshtein, L. Presnyakov, and I. Sobelman, Zh. Eksp. Teor. Fiz. 45, 2015 (1963) [Sov. Phys.—JETP 18, 1383 (1964)].
[29]R. Abrines and I. C. Percival, Proc. Phys. Soc. London 88, 873 (1966).
[30]M. E. Rudd, Phys. Rev. A 20, 787 (1979).
[31]A. Salop and J. Eichler, J. Phys. B 12, 257 (1979).
[32]K. H. Berkner, W. G. Graham, P. V. Pyle, A. S. Schlachter, J. W. Stearns, and R. E. Olson, J. Phys. B 11, 875 (1978).
[33]K. H. Berkner, W. G. Graham, R. V. Pyle, A. S. Schlachter, and J. W. Stearns (private communication).
[34]L. I. Pivovar, Yu. Z. Levchenko, and G. A. Krivonosov, Zh. Eksp. Teor. Fiz. 59, 19 (1970) [Sov. Phys.—JETP 32, 11 (1971)].
[35]J. T. Park, J. E. Aldag, J. E. George, and J. L. Peacher, Phys. Rev. A 14, 608 (1976).
[36]T. J. Morgan, J. Geddes, and H. B. Gilbody, J. Phys. B 6, 2118 (1973).
[37]T. Kondow, R. J. Girnius, Y. P. Chong, and W. L. Fite, Phys. Rev. A 10, 1167 (1974).
[38]C. E. Theodosiou, Phys. Rev. A 22, 2556 (1980).
[39]M. B. Shah, T. V. Goffe, and H. B. Gilbody, J. Phys. B 11, L233 (1978).
[40]D. H. Crandall, R. A. Phaneuf, and F. W. Meyer, Phys. Rev. A 19, 504 (1979).
[41]L. D. Gardner, J. E. Bayfield, P. M. Koch, H. J. Kim, and P. H. Stelson, Phys. Rev. A 16, 1415 (1977).
[42]F. W. Meyer, R. A. Phaneuf, H. J. Kim, P. Hvelplund, and P. H. Stelson, Phys. Rev. A 19, 515 (1979).
[43]K. H. Berkner, W. G. Graham, R. V. Pyle, A. S. Schlachter, and J. W. Stearns, Phys. Lett. 62A, 407 (1977).
[44]T. P. Grozdanov and R. K. Janev, Phys. Rev. A 17, 880 (1978).
[45]R. E. Olson and A. Salop, Phys. Rev. A 14, 579 (1976).
[46]J. K. M. Eichler, Phys. Rev. A 23, 498 (1981).